Received: 12 June 2018 | Revised: 5 September 2018 | Accepted: 11 October 2018
DOI: 10.1002/cpe.5074

WILEY

SPECIAL ISSUE PAPER

Pansharpening multispectral remote-sensing images with guided filter for monitoring impact of human behavior on environment

Qilei Li[1] | Xiaomin Yang[1] | Wei Wu[1] | Kai Liu[2] | Gwanggil Jeon[3,4]

[1]College of Electronics and Information Engineering, Sichuan University, Chengdu, China
[2]College of Electrical and Engineering Information, Sichuan University, Chengdu, China
[3]School of Electronic Engineering, Xidian University, Xi'an, China
[4]Department of Embedded Systems Engineering, Incheon National University, Incheon, South Korea

Correspondence
Wei Wu, College of Electronics and Information Engineering, Sichuan University, Chengdu 610064, China.
Email: wuwei@scu.edu.cn

Funding information
National Natural Science Foundation of China, Grant/Award Number: 61473198, 61701327, and 61711540303; Science Foundation of Sichuan Science and Technology Department, Grant/Award Number: 2018GZ0178

Summary

Human behavior would lead to a significant impact on the environment. By monitoring the environment, we can indirectly monitor human behavior. Remote sensing (RS) technology provides a large number of multispectral (MS) images. When combining the Internet of things (IoT) technology, those images can be used for human behavioral monitoring. However, due to the limitation of the optical sensors embedded in satellites, the spatial resolution of MS image is relatively low, which poses a huge problem for further understanding these images. Pansharpening, also known as multisensor image fusion, aims to sharp an MS image to a high-resolution multisensor image (HMS) by integrating a corresponding high-resolution panchromatic (PAN) image. By doing so, the redundancy among big data can be effectively reduced. Traditional Intensity-Hue-Saturation (IHS)–based methods often suffer from spectral distortion. To address this problem, a novel pansharpening method is proposed in this paper. Different from those traditional IHS methods, the proposed method first decomposes MS and PAN into high-frequency-component (HFC) and low-frequency-component (LFC), respectively. Then, the guided filter (GF) is utilized to enhance the spectral information on the detail map. Furthermore, the detail map is refined according to the adaptive coefficients for each band of MS. By performing experiments, we demonstrate the proposed method can obtain satisfying results in both visual quality and object assessment among existing methods.

KEYWORDS

behavioral monitoring, guided filter (GF), Intensity-Hue-Saturation (IHS) transform, pansharpening, spectral information

1 | INTRODUCTION

Remote sensing (RS) technology is widely used to predict abnormal scene, monitor environmental changes, and forecast natural disasters for human behavioral monitoring,[1] as shown in Figure 1. Multispectral images can be obtained from different satellites, such as Pleiades, Spot-6, and Worldview-2, etc. However, due to the limitation of optical sensors embedded in satellites, we can only obtain multispectral (MS) images[2] with low spatial resolution and panchromatic (PAN) images with low spectral resolution, which poses a huge problem for further understanding these images. Therefore, it is highly desired to obtain an MS image with both high spatial and spectral resolution. To make full use of the information from those two categories images, pansharpening technology,[3] also known as multisensor image fusion technology, can fuse MS image with PAN image to obtain a high-resolution multisensor image (HMS).

To date, numerous pansharpening methods have been proposed. The basic protocol of those methods is to merge the spatial structure from PAN image with the corresponding MS image to obtain an HMS image. According to different processing mode, these methods can be roughly divided into two categories,[4] ie, multi-resolution-analysis (MRA) methods and component-substitution (CS) methods, as shown in Figure 2.

MRA methods are mainly based on ARSIS theory.[5] This theory assumes that, compared with the HMS image, the MS image loses a lot of spatial information, while the lost information exists in the HFC of PAN image. Therefore, the basic protocol of MRA methods is to decompose

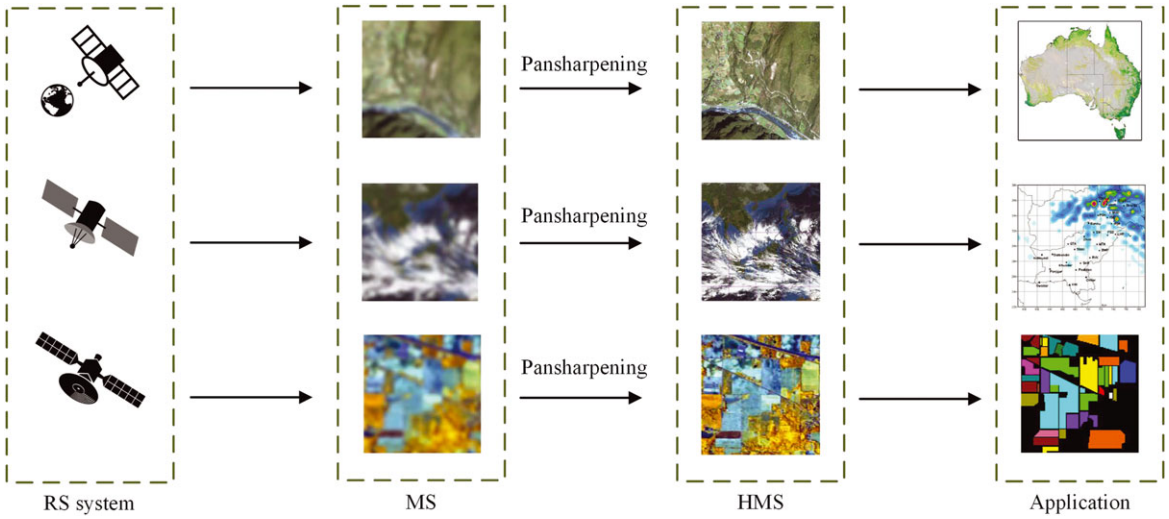

FIGURE 1 Pansharpening multispectral images for human behavior monitoring

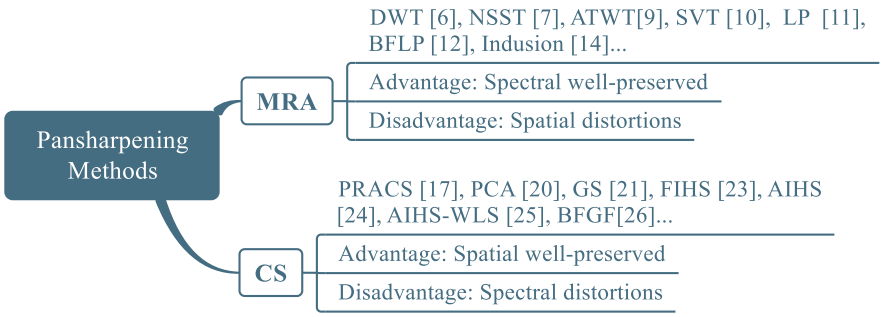

FIGURE 2 Pansharpening methods

PAN image into multi-scale to extract spatial detail and merge it into MS image to obtain the HMS image. To decompose PAN image, many image processing tools have been applied, such as decimated wavelet transform (DWT),[6] nonsubsampled shearlet transform (NSST),[7] undecimated wavelet transform (UDWT),[8] "à trous" wavelet transform (ATWT),[9] support value transform (SVT),[10] Laplacian pyramid (LP),[11] bilateral filter (BFLP),[12] intrinsic image decomposition (IID),[13] and indusion method (Indusion).[14] Recently, the development of deep learning brings another solution for pansharpening. Scarpa et al[15] used the convolutional network to learn the mapping between the fused image and the source images. Vivone et al[16] used deconvolution algorithm to estimate the spatial filter, which can extract the in each band.

Those MRA methods can produce HMS images with high spectral quality. However, these MRA methods always not fully consider the adaptation between the spatial information in PAN image and spectral information in the corresponding MS image, leading to the pansharpened HMS images constantly suffer from spatial distortion, such as ringing phenomenon and local blurring.

Different from MRA methods, CS methods pansharpen MS images by substituting one or more specific component(s) in MS image with the corresponding component(s) in PAN image. Among CS methods, the component substitution methods based on partial replacement (PRACS),[17] intensity-hue-saturation (IHS),[18] principal component analysis (PCA),[19,20] and Gram-Schmidt (GS)[21] are the most well-known pansharpening methods. Among the CS methods, IHS methods are a kind of representative methods. In the original IHS[22] method, MS image is transformed from RGB space into IHS space; then, the intensity component *I* is replaced by the corresponding PAN image. Finally, the HMS image is obtained by transforming the new image from IHS space to RGB space. This method is widely employed due to its simple, efficient, and convenient. Though it can achieve high spatial quality, it often suffers from serious spectral distortion. Besides, this method can only pansharpen three bands, ie, R, G, and B, while most MS images have another band, ie, near-infrared (NIR). In other words, the IHS method doesn't fully use information of MS images. To overcome these drawbacks, various evolutive IHS methods have been developed. Tu et al[23] proposed a fast IHS (FIHS) pansharpening method, which can pansharpen four bands of MS image, and efficiently reduce computational cost. To further reduce spectral distortion, Rahmani et al[24] proposed an adaptive IHS (AIHS) pansharpening method, which can calculate the coefficient α_i for each band adaptively. Similar with other CS methods, HMS images obtained by AIHS method often suffer from spectral distortion. Based on AIHS, Song et al[25] combined weighted least squares with AIHS (AIHS-WLS) to eliminate the influence of LFC and fuse the MS image adaptively. Jian et al[26] utilized bilateral filter (BFGF) to decompose source image and utilized guided filter to refine the HMS image. Chen and Zhang[27] used an evolutionary algorithm to optimize fused result based on IHS transformation.

Generally, HMS images obtained from these CS methods can achieve better spatial resolution but slightly poor in preserving spectral information.

In general, HMS images obtained by MRA methods often lead to spatial distortions, while HMS images obtained by CS methods often lead to spectral distortion. Therefore, it is very important to balance spatial distortions and spectral distortions. To achieve this goal, a novel pansharpening method is proposed in this paper. In the proposed method, first, MS image and PAN image are decomposed into HFC and LFC by using GF.[28] By AIHS method, the high frequency of intensity component I^H of HFC can be calculated. Then, the initial detail map is obtained by substituting I^H band with PAN^H. By doing so, the spatial information is enhanced. Moreover, GF is utilized to extract spectral information from MS image and to merge the information into the initial detail map. To further refine the spectral information-enhanced detail map, adaptive coefficients calculated according to spectral signature is applied. Finally, HMS image is generated via merging the refined detail map into MS image. Compared with traditional AIHS methods, such as AIHS,[24] AIHS-WLS,[25] BFGF,[26] etc, there are two major contributions.

1. Traditional AIHS methods fuse multispectral image by replacing I component with PAN image in both HFC and LFC. This often leads to spectral distortion in HMS image. To address this problem, we utilize GF to eliminate the influence of LFC. By doing so, we efficiently reduce spectral distortion. The fused HMS image by the proposed method can achieve better visual effects.
2. Traditional AIHS methods does not fully use the spectral information from MS image, thus often increase spectral distortion. To address this problem, GF is utilized to extract spectral information from MS image, and inject the spectral information into the detail map. By doing so, the special information is enhanced. Thus, the HMS image contains more spectral information.

To validate the proposed method, several experiments are performed. By performing experiments, we demonstrate that our method can obtain satisfying results in both visual quality and objective assessments among existing methods.

The remained paper is organized as follows. In Section 2, GF and AIHS method are briefly reviewed. Section 3 describes the proposed pansharpening method in detail. Section 4 analyzes the experimental results. Finally, Section 5 concludes this paper.

2 | RELATED WORK

In this section, basic theories of GF and AIHS methods are briefly reviewed.

2.1 | Guided filter

GF is a powerful image filter which has been used in many computer vision tasks such as colorization, image fusion, image matting, and up-sampling. It filters the input image by merging the information from the corresponding guidance image. The guidance image can be the input image itself or a different image. When the guidance image is the input image, GF acts as an edge-preserving filter. It can preserve the strong edges of the input image. When the guidance image is a different image, GF will extract the structure information from guidance image and merge the structure information into the input image. Figure 3 shows an illustration of the guided filtering process. The applications of the guided filter are shown in Figure 4. In this paper, the two applications of GF are both utilized. First, it is utilized to decompose MS image and PAN image into LFC and HFC, respectively. Second, to enhance the spectral information, it is utilized to extract spectral information from MS image.

GF filters input image in a local window by a linear transform. In more detail, given an input image I and a guidance image G, the output image O can be regarded as the linear transform of G at pixel p, where p is the center of a local window ω_k. Within a local window ω_k, this operation can be expressed as Equation (1)

$$O_i = a_k G_i + b_k \quad \forall i \in \omega_k, \tag{1}$$

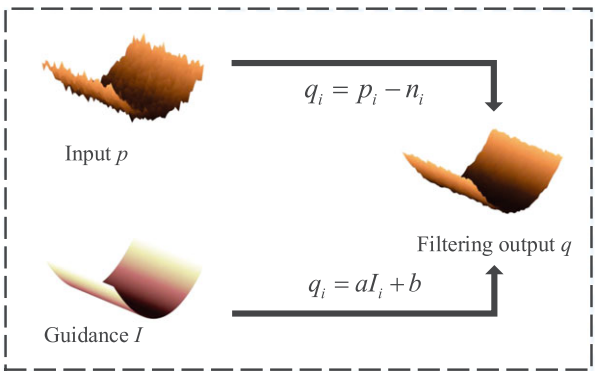

FIGURE 3 Illustrations of the guided filtering process

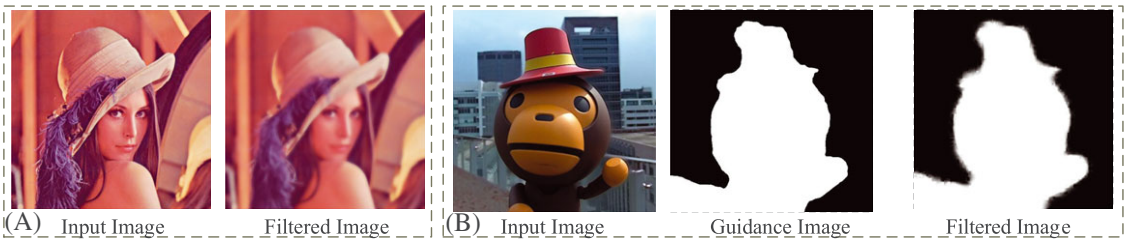

FIGURE 4 Two applications of the guided filter. (A) When the input image and the guidance image are the same image, GF will smooth the input image. (B) When the input image[29] and the guidance image are different images, GF will extract the structure information from the guidance image and merge the structure information into the input image

where a_k and b_k are two constant linear coefficients in ω_k; they can be calculated by minimizing Equation (2). ω_k is a window with size $(2r + 1) \times (2r + 1)$; O_i is the output of ω_k

$$E(a_k, b_k) = \sum_{i \in \omega_k} \left((a_k G_i - I_i)^2 + \lambda a_k^2 \right), \tag{2}$$

where λ is the regularization factor set manually. By solving Equation (3), a_k and b_k can be calculated

$$\begin{aligned} a_k &= \frac{\frac{1}{|\omega|} \sum_{i \in \omega_k} G_i I_i - \mu_k \bar{I}_k}{\delta_k + \epsilon} \\ b_k &= \bar{I}_k - a_k \mu_k, \end{aligned} \tag{3}$$

where μ_k and δ_k denote the mean and the variance of G in ω_k, $|\omega|$ is total pixel number of ω_k, and $\bar{P}_k$ denotes mean of P_k. Then, the filtered image O can be obtained by averaging all the overlapping O_i, while O_i can be obtained via solving Equation (1).

It is worth noting that the value of O_i is changed when calculating it in different local window ω_k. To avoid this issue, all possible values of a_k and b_k are averaged first. Thus, the filtered output can be rewritten as Equation (4)

$$O_i = \bar{a}_i G_i + \bar{b}_i. \tag{4}$$

In this paper, the procedure of GF is denoted as Equation (5)

$$O = GF(I, G, r, \epsilon). \tag{5}$$

2.2 | AIHS methods

IHS method fuse MS images by replacing the I band with PAN image, as shown in Figure 5. This can be expressed as Equation (6)

$$HMS_i = MS_i + \eta_i (P - I), \tag{6}$$

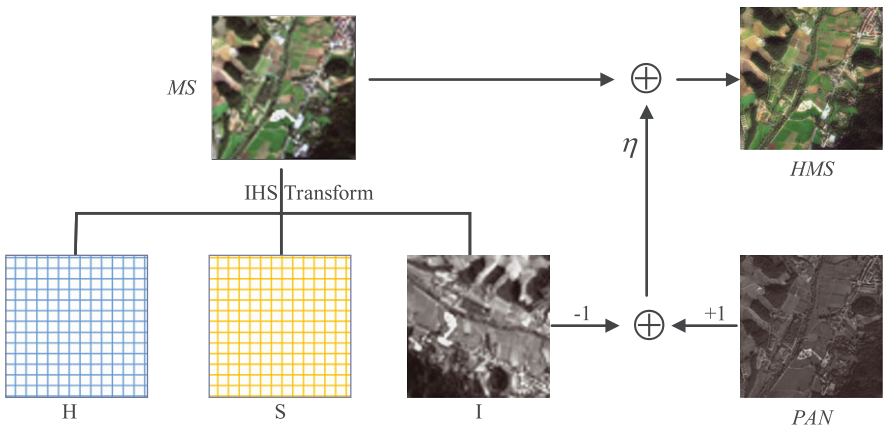

FIGURE 5 IHS pansharpening method replaces *I* component with PAN image

where P denotes PAN image. η_i denotes gain coefficients for each band. I represents the intensity channel of MS image, which can be calculated according follow equation:

$$I = \sum_{i=1}^{N} \alpha_i MS_i, \tag{7}$$

where N denotes the number of spectral bands in MS image, α_i is the weighting coefficient for i_{th} band.

The original IHS method can only sharpen MS image in three color channels, ie, R, G, and B channels, ignoring the NIR channel. To overcome this problem, Tu et al[23] proposed the FIHS method, fully used the four bands of MS image. The weighting coefficient α_i in FIHS method is fixed as $1/N$. However, the pansharpening result obtained via FIHS method still suffers serious spectral distortion. To further reduce spectral distortion, AIHS method can calculate the coefficient $\alpha_i, (i = 1, 2, 3, 4)$ for each band adaptively via solving Equation (8)

$$\min_{\alpha_i, \ldots, \alpha_N} \left\| P - \sum_{i=1}^{N} \alpha_i MS_i \right\|^2 \qquad s.t. \alpha_1 \geq 0, \ \ldots, \alpha_N \geq 0. \tag{8}$$

3 | PROPOSED METHOD

As is shown in Figure 6, the proposed method consists of three phases.

1. Decomposing source images and obtaining an initial detail map;
2. Enhancing spectral information of the initial detail map; and
3. Refining spectral information-enhanced detail map adaptively.

Given a pair of pretreated satellite images consists of an MS image and a PAN image (the pretreating process is in Section 4), first, MS image and PAN image are decomposed into HFC and LFC by using GF, respectively. Then, the initial detail map is obtained by subtracting PAN image with I^H band. To enhance spectral information in the initial detail map, spectral information is extracted from MS image and merged into the initial detail map by using GF. To further refine the spectral information-enhanced detail map, adaptive coefficients are applied. Finally, the HMS image is generated via merging the refined detail map into MS image. The following sections will explain these steps in detail.

3.1 | Decomposing source images and obtaining initial detail map

In the first phase, GF is utilized to decompose PAN image and MS image into HFC and LFC according to Equation (9), respectively,

$$\begin{aligned} MS_i^L &= GF(MS_i, MS_i, r_1, \epsilon_1) \qquad i = 1, 2, 3, 4 \\ PAN^L &= GF(PAN, PAN, r_1, \epsilon_1), \end{aligned} \tag{9}$$

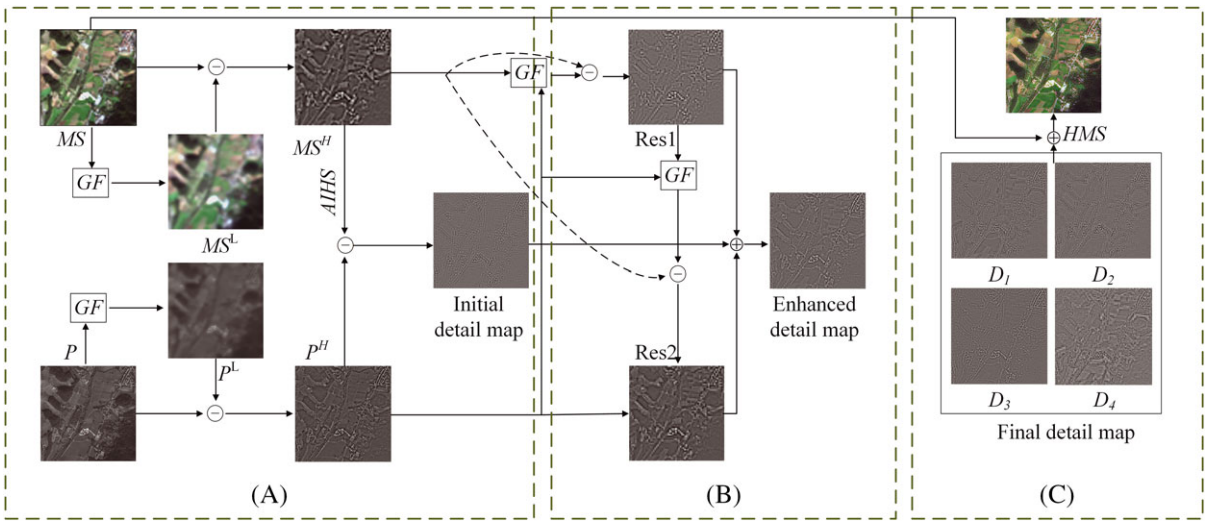

FIGURE 6 The overall framework of the proposed method. A, Decomposing source images and obtaining initial detail map; B, Enhancing spectral information of initial detail map; C, Refining spectral information-enhanced detail map adaptly

where $GF(\bullet)$ denotes GF operation. The two original images are denoted as MS and PAN. The LFC of MS and PAN are denoted as MS^L and PAN^L, respectively. r_1, ϵ_1 denote radius and regularization factor of GF, respectively. Therefore, the HFC of MS and PAN can be obtained as follows:

$$\begin{aligned} MS_i{}^H &= MS_i - MS_i{}^L \qquad i = 1, 2, 3, 4 \\ PAN^H &= PAN - PAN^L. \end{aligned} \tag{10}$$

To reduce spectral distortion, the LFC is eliminated. We directly estimate the initial detail map from the intensity band of MS^H and PAN^H. According to Equation (8), the AIHS method is used to calculate the adaptive coefficient α as Equation (11)

$$\min_{\alpha_i, \ldots, \alpha_4} \left\| P^H - \sum_{i=1}^{4} \alpha_i MS_i{}^H \right\|^2 \qquad s.t. \alpha_1 \geq 0, \ldots, \alpha_4 \geq 0. \tag{11}$$

With the adaptive coefficient α, the HFC of intensity band can be obtained via Equation (12)

$$I^H = \sum_{i=1}^{4} \alpha_i MS_i{}^H, \tag{12}$$

where I^H denotes the HFC of I.

The initial detail map D_{init} measures the difference between I^H and PAN^H. It can be obtained as follows:

$$D_{init} = PAN^H - I^H. \tag{13}$$

3.2 | Enhancing spectral information of initial detail map

Comparing with the original MS image, the initial detail map contains more spatial information. However, it still suffers from spectral distortion due to the I^H band is subtracted. To address this problem, GF is utilized to extract spectral information from MS image. The residuals of the filtered MS image and the original MS image contains not only spatial structure but also spectral information. This can be expressed as Equation (14)

$$\begin{aligned} MS_{O_1}^H &= GF\left(PAN^H, MS^H, r_2, \epsilon_2\right) \\ Res_1 &= MS^H - MS_{O_1}^H \\ MS_{O_2}^H &= GF\left(PAN^H, Res1, r_2, \epsilon_2\right) \\ Res_2 &= MS^H - MS_{O_2}^H, \end{aligned} \tag{14}$$

where Res_1 and Res_2 denote the two-level residuals, $MS_{O_1}^H$ and $MS_{O_2}^H$ denote the two-level filtered MS^H images, and r_2 and ϵ_2 denote the radius and regulation factor used in this phase, respectively.

Those residuals are utilized to enhance the spectral information of the initial detail map to obtain the spectral information-enhanced detail map. This can be expressed as Equation (15)

$$D_{ehcd} = D_{init} + Res_1 + Res_2, \tag{15}$$

where D_{ehcd} denotes the spectral information-enhanced detail map.

3.3 | Refining spectral information-enhanced detail map adaptively

In this phase, the D_{ehcd} is adaptively refined toward the different channel. Due to the D_{ehcd} and MS image having same spectral signatures, the adaptive coefficient α doesn't need to be updated. To stress the spatial structure information, the I^H obtained as Equation (16) band should be closed to PAN image

$$\overline{I^H} = \sum_{i=1}^{4} \alpha_i HMS_i = \sum_{i=1}^{4} \alpha_i (MS_i + D_i), \tag{16}$$

where $\overline{I^H}$ denotes the intensity band of HMS^H.

Therefore, the refined detail map can be obtained by solving the following equation:

$$\min_{\overline{D_i}} \left\| P^H - \sum_{i=1}^{4} \alpha_i \left(MS_i{}^H + \overline{D_i} \right) \right\|^2 \qquad i = 1, 2, 3, 4, \tag{17}$$

where $\overline{D_i}$ denotes the refined detail map.

Once the refined detail map is obtained, the HMS can be generated by solving Equation (18)

$$HMS_i = MS_i + \overline{D_i}. \tag{18}$$

FIGURE 7 Remote-sensing images used in this paper. (A) and (B) are captured by Spot-6. (C) is captured by Worldview-2. (D) is captured by Pleiades. A, Vegetation; B, Cropland; C, Mountain; D, Urban

4 | EXPERIMENTAL RESULT AND ANALYSIS

To validate the effectiveness of the proposed method, experiments are performed on three satellites datasets, namely, Spot-6, Worldview-2, and Pleiades, respectively. Those test images are shown in Figure 7. The scenes described in these images are village, cropland, mountain, and urban. The MS images from Spot-6 and Pleiades satellites contain four bands, ie, R, G, B, and NIR. The MS images from WorldView-2 satellite contain 8 bands, but only R, G, B, and NIR bands are adopted.

4.1 | Parameters setup

The size of original MS images are 256 × 256, and the size of PAN images are 1024 × 1024. According to Wald's criterion,[30] to set the original MS images as reference, the original MS and PAN image are first downsampled with a factor of 1/4 by bicubic interpolation. The downsampled MS and PAN image are denoted as DMS and DPAN, respectively. Then, the DMS is upsampled to the original size with a factor of 4 by bicubic interpolation. The upsampled DMS is denoted as UMS. By doing so, the original MS can servers as a reference to the pansharpening result of UMS and DPAN. To decompose source images, r_1 and ϵ_1 are set to 2 and 0.1, respectively. To extract spectral information, r_2 and ϵ_2 are set to 2 and 0.1, respectively.

Besides, eight popular pansharpening methods are compared with the proposed method. Those comparison methods are SVT,[10] BFLP,[12] Indusion,[14] PRACS,[17] PCA,[19] GS,[21] FIHS,[23] AIHS,[24] and AIHS-WLS,[25] respectively. Parameters of those comparative methods are set according to the relevant publications.

4.2 | Quality evaluation

Nine metrics are employed to evaluate the proposed method objectivity.

1. Correlation Coefficient (CC)[31] calculates the correlation between the reference image and fused result. The large value denotes the fused result is closer to the reference image. The ideal value is 1.
2. Universal Image Quality Index (UIQI)[32] reflects the correlation loss, brightness distortion, and contrast distortion of the pansharpening result. The larger value denotes the better pansharpening result. The ideal value is 1.
3. Relative Dimensionless Global Error in Synthesis (ERGAS)[33] calculates the global quality of the fused image. The ideal value is 0.
4. Relative Average Spectral Error (RASE)[34] measures the performance of each band in fused image. The ideal value is 0.
5. Root Mean Square Error (RMSE) is used to compare the difference between two images by calculating the difference between pixel values. The smaller value denotes the lesser difference. The ideal value is 0.
6. Spectral Information Divergence (SID)[35] measures the discrepancy between spectra. The ideal value is 0.
7. Quality with No Reference (QNR)[36] can evaluate the quality of the fused image without reference. It consists of three parts, which are spectral distortion index λ_d, spatial distortion index λ_s, and a global QNR index, respectively. For the global QNR index, the larger value denotes the better fusion result, and the ideal value is 1.
8. λ_d is a sub-metric of QNR. It is used to measure the spectral distortion. The smaller values denote the better fusion result. The ideal value of λ_d is 0.
9. λ_s is another sub-metric of QNR. It is used to measure the spatial distortion. The smaller values denote the better fusion result. The ideal value of λ_s is 0.

For all the metrics, the best results are shown in bold, and the second best results are underlined.

4.3 | Result and comparison

Experiments are first performed on Village images captured by Spot-6 satellite. The pansharpening results are shown in Figure 8. The pansharpening results obtained by PRACS, PCA, FIHS, and BFLP suffer serious spectral distortion, The color of the green ornament at the top

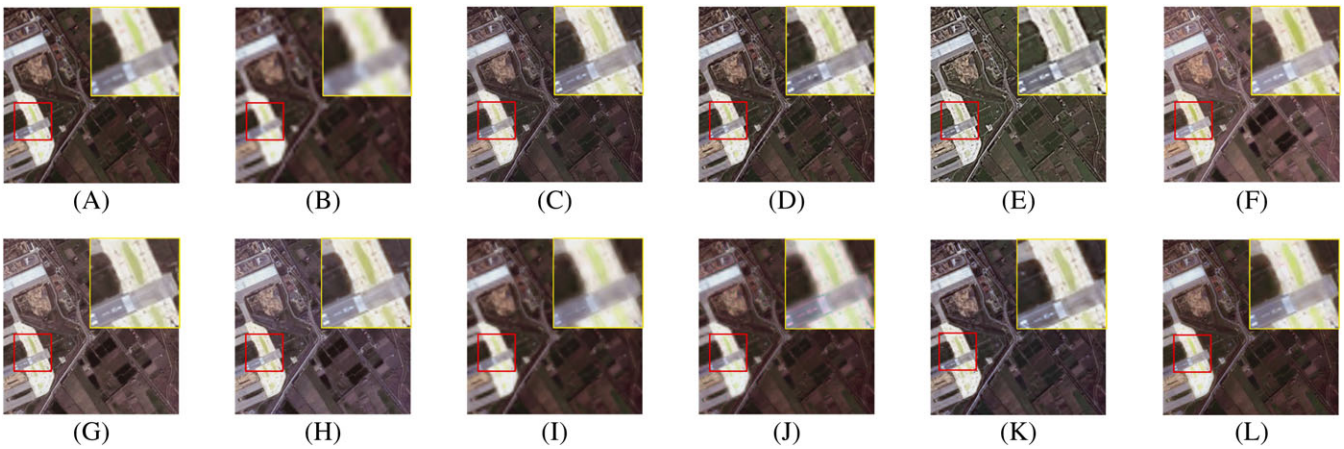

FIGURE 8 Pansharpening results of Village image captured by Spot-6 satellite. (A) Original MS image, also names reference. (B) Upsampled DMS image. (C) to (L) Pansharpening results by SVT, Indusion, PRACS, PCA, GS, FIHS, AIHS, AIHS-WLS, BFLP, and the proposed method, respectively. A, Referance; B, UMS; C, SVT; D, Indusion; E, PRACS; F, PCA; G, GS; H, FIHS; I, AIHS; J, AIHS-WLS; K, BFLP; I, Proposed

TABLE 1 Quantitative metrics for Village image

Methods	CC	UIQI	ERGAS	RASE	RMSE	SID	QNR	D_λ	D_s
Reference	1	1	0	0	0	0	1	0	0
SVT	0.9707	0.9697	2.0359	8.9954	30.1251	**0.0085**	0.9136	0.0568	0.0314
BFLP	0.9692	0.9674	2.0916	9.5300	31.9157	0.0105	0.8899	0.0689	0.0443
Indusion	0.9602	0.9601	2.5310	10.9428	36.6471	0.0396	0.9574	0.0379	**0.0049**
PRACS	0.9295	0.9192	4.1857	14.7769	49.4872	0.0866	0.9145	0.0410	0.0465
PCA	0.9287	0.8607	4.2643	15.7444	52.7273	0.0183	0.9155	0.0649	0.0210
GS	0.9518	0.9453	2.9953	11.7356	39.3022	0.0268	0.9475	0.0192	0.0340
FIHS	0.9479	0.9405	2.8563	11.7230	39.2600	0.0217	0.9332	0.0320	0.0360
AIHS	0.9821	0.9807	1.7382	7.4389	24.9124	0.0101	**0.9816**	**0.0031**	0.0153
AIHS-WLS	0.9814	0.9805	1.7318	7.4638	24.9958	0.0092	0.9618	0.0194	0.0192
Proposed	**0.9845**	**0.9843**	**1.5816**	**7.0153**	**23.4939**	0.0197	0.9739	0.0083	0.0179

of the building and the color of the farmland have been changed. This is because the above method loses a lot of spectrum information in the process of decomposing the image and fusing the image. The AIHS and AIHS-WLS methods fail to enhance the spatial information. The edge of the green building is still blurred. This is because the AIHS and AIHS-WLS methods fail to stress spatial information from PAN image. Though spatial information of the result obtained by SVT method is enhanced, it loses much spectral information is lost. This is mainly due to the SVT method fails to balance the spectral information and spatial information. The pansharpening result obtained by proposed method is the closest one to the reference. It not only fully uses the spatial information from PAN image but also preserves most spectral information of the UMS image. The quantitative metrics for Village image is shown in Table 1. The proposed method achieves the best performance in CC, UIQI, ERGAS, RASE, and RMSE. It achieves the second best performance in QNR and D_λ. Combining visual effects and evaluation indicators, we demonstrate the proposed method can preserve spatial structure and enhance the spectral information.

Another experiment is performed on Cropland image captured by Spot-6 satellite. Most of the image is covered with farmlands and farmhouses. The pansharpening results are shown in Figure 9. Results obtained by BFLP, PCA, and AIHS-WLS methods lose a lot of spectral information. This is mainly caused by these methods fail to properly fuse the decomposed images. This leads to the change of overall color. The PRACS method does not replace the property partial of the source images, leading to obvious artifact around the farmhouses. AIHS and proposed method can produce the fused images, which have a similar visual effect. From the enlarged images, we can see that the proposed method can produce a pansharpened result, which is even more clear than the reference. The objective evaluation for this experiment is shown in Table 2. The proposed method obtains the best performance in six metrics and the second best performance in two metrics. The subjective visual effect is consistent with the object evaluation metrics. Thus, the effectiveness of the proposed method is demonstrated.

The pansharpening results of Mountain image captured by Worldview-2 satellite is shown in Figure 10. It can be found that the pansharpening result obtained by PCA method suffers serious color distortion, and the red hills turn green. This is because PCA loses a lot of information during dimension reduction and dimensional recovery. Moreover, the pansharpening results obtained by Indusion and FIHS method also suffered from a slight spectral distortion. From the enlarged image, the pansharpening results obtained by PAC, FIHS, and Indusion are obvious suffer spectral distortion. The color of the green forest becomes brown. Compared with other pansharpening methods, the proposed method and the BFLP method can produce high-quality HMS images, which are the closest to the reference. The proposed method fully uses the spatial information

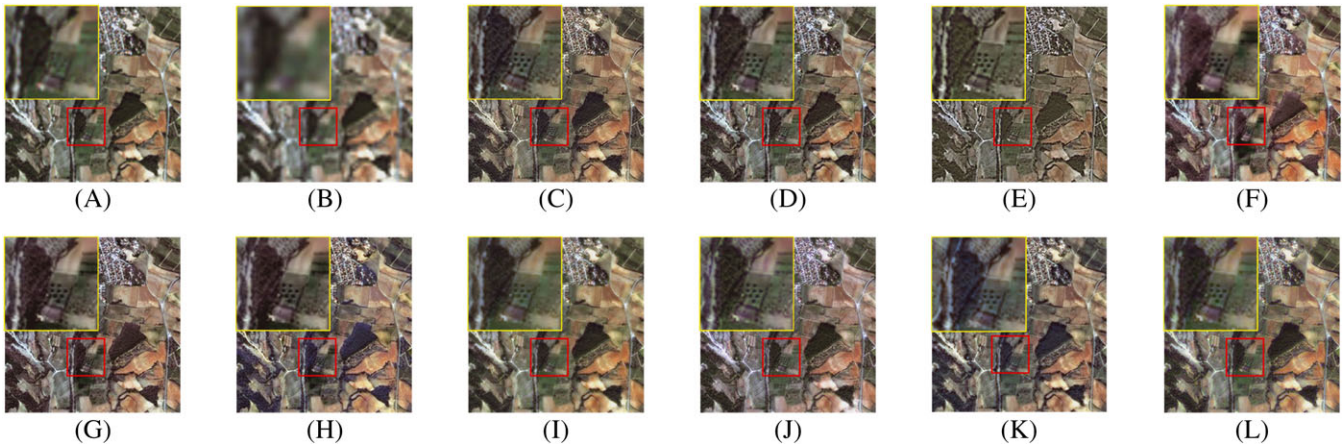

FIGURE 9 Pansharpening results of Cropland image captured by Spot-6 satellite. (A) Original MS image, also names reference. (B) Upsampled DMS image. (C) to (L) Pansharpening results by SVT, Indusion, PRACS, PCA, GS, FIHS, AIHS, AIHS-WLS, BFLP, and the proposed method, respectively. A, Referance; B, UMS; C, SVT; D, Indusion; E, PRACS; F, PCA; G, GS; H, FIHS; I, AIHS; J, AIHS-WLS; K, BFLP; L, Proposed

TABLE 2 Quantitative metrics for Cropland image

Methods	CC	UIQI	ERGAS	RASE	RMSE	SID	QNR	D_λ	D_s
Reference	1	1	0	0	0	0	1	0	0
SVT	0.9051	0.8946	2.5976	11.2999	30.7732	0.0117	0.8240	0.1240	0.0594
BFLP	0.9174	0.8998	2.5777	11.8089	32.1596	0.0093	0.7871	0.1427	0.0819
Indusion	0.9050	0.9046	2.7898	11.8877	32.3742	0.0231	0.9309	0.0488	**0.0214**
PRACS	0.8483	0.8009	5.2560	18.2409	49.6758	0.0556	0.8107	0.1063	0.0930
PCA	0.8730	0.7732	3.6436	14.2988	38.9402	0.0199	0.8068	0.1430	0.0587
GS	0.9080	0.8927	2.7526	11.5020	31.3238	0.0171	0.9598	0.0102	0.0302
FIHS	0.8883	0.8728	2.6542	11.4394	31.1532	0.0117	0.9431	0.0243	0.0334
AIHS	**0.9445**	0.9316	2.0710	9.4643	25.7742	**0.0085**	0.9429	0.0127	0.0449
AIHS-WLS	0.9395	0.9339	2.1288	9.5519	26.0129	0.0100	0.9215	0.0495	0.0305
Proposed	0.9396	**0.9387**	**2.0345**	**9.2282**	**25.1315**	0.0113	**0.9667**	**0.0080**	0.0255

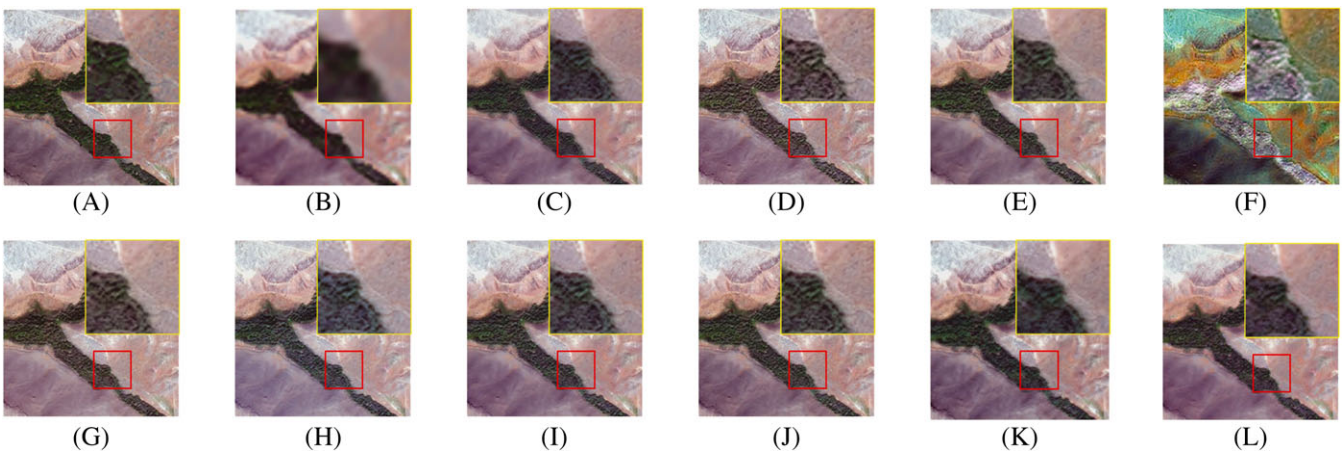

FIGURE 10 Pansharpening results of Mountain image captured by Worldview-2 satellite. (A) Original MS image, also names reference. (B) Upsampled DMS image. (C) to (L) Pansharpening results by SVT, Indusion, PRACS, PCA, GS, FIHS, AIHS, AIHS-WLS, BFLP, and the proposed method, respectively. A, Referance; B, UMS; C, SVT; D, Indusion; E, PRACS; F, PCA; G, GS; H, FIHS; I, AIHS; J, AIHS-WLS; K, BFLP; I, Proposed

from PAN image, and it handles the trade-off among spectral information and spatial information efficiently. To further validate the effectiveness of the proposed, the objective evaluation metrics are shown in Table 3. From the table, it can be seen the proposed method achieves the best performance in seven indices and the second best performance in one index. Combined with subjective visual effects and objective evaluation indicators, the superiority of the proposed is verified.

Experiment is performed on Urban image captured by Pleiades satellite. As is shown in Figure 11, the PARCS, PCA, and BFLP suffer severe spectral distortion. In detail, the results of PARCS and BFLP are slightly yellowish, which is caused by the inappropriate image decomposition

TABLE 3 Quantitative metrics for Mountain image

Methods	CC	UIQI	ERGAS	RASE	RMSE	SID	QNR	D_λ	D_s
Reference	1	1	0	0	0	0	1	0	0
SVT	0.9642	0.9623	1.7831	8.4550	5.9243	0.0062	0.9659	0.0090	0.0253
BFLP	**0.9693**	**0.9692**	**1.6400**	**7.7266**	**5.4139**	**0.0038**	0.9557	0.0152	0.0296
Indusion	0.9438	0.9437	2.2020	9.6981	6.7953	0.0349	0.9667	0.0093	0.0242
PRACS	0.9631	0.9620	1.8225	8.6707	6.0754	0.0110	0.9694	0.0061	0.0246
PCA	0.1779	0.1549	6.7512	29.2188	20.4731	0.1161	0.8518	0.0943	0.0595
GS	0.9567	0.9534	1.9853	8.8620	6.2095	0.0242	0.9899	0.0084	**0.0017**
FIHS	0.9527	0.9486	1.9268	8.6500	6.0609	0.0140	0.9778	0.0181	0.0041
AIHS	0.9637	0.9622	1.7241	7.9272	5.5545	0.0114	0.9865	**0.0056**	0.0080
AIHS-WLS	0.9658	0.9650	1.6982	7.8646	5.5106	0.0103	0.9862	0.0073	0.0065
Proposed	0.9676	0.9672	1.6693	7.8259	5.4835	0.0076	**0.9910**	0.0057	0.0033

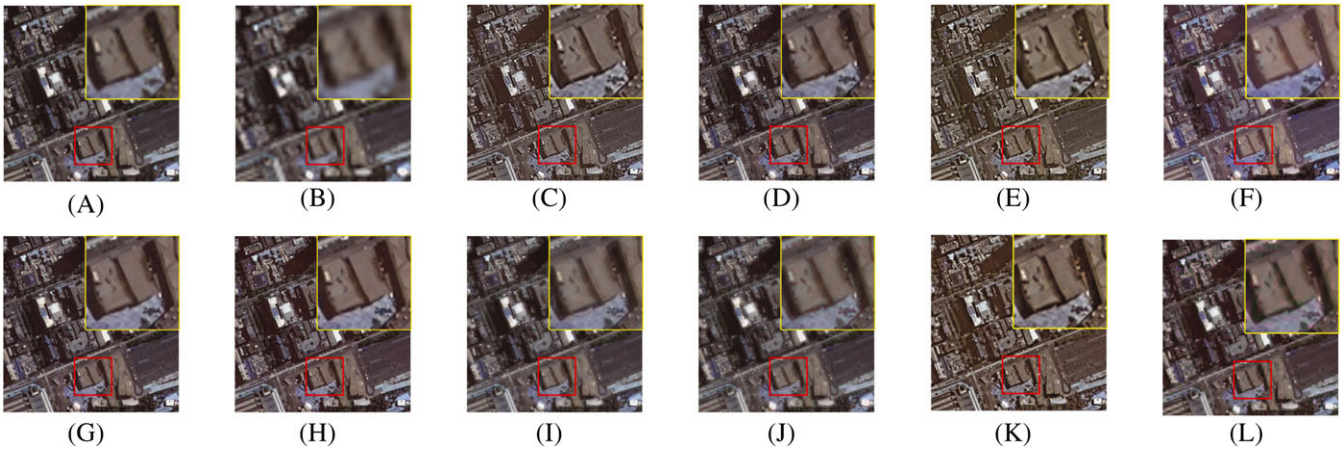

FIGURE 11 Pansharpening results of Urban image captured by Pleiades satellite. (A)Original MS image, also names reference. (B) Upsampled DMS image. (C) to (L) Pansharpening results by SVT, Indusion, PRACS, PCA, GS, FIHS, AIHS, AIHS-WLS, BFLP, and the proposed method, respectively. A, Referance; B, UMS; C, SVT; D, Indusion; E, PRACS; F, PCA; G, GS; H, FIHS; I, AIHS; J, AIHS-WLS; K, BFLP; I, Proposed

TABLE 4 Quantitative metrics for Urban image

Methods	CC	UIQI	ERGAS	RASE	RMSE	SID	QNR	D_λ	D_s
Reference	1	1	0	0	0	0	1	0	0
SVT	0.8584	0.8299	8.9719	35.5038	88.5820	0.0756	0.8659	0.0583	0.0805
BFLP	0.8706	0.7965	10.5293	43.3900	108.2580	0.0772	0.8115	0.0567	0.1397
Indusion	0.9205	0.9195	5.5234	21.3901	53.3682	0.0489	0.9636	**0.0054**	0.0311
PRACS	0.8285	0.7888	10.4707	41.1312	102.6224	0.0775	0.8676	0.0456	0.0910
PCA	0.9102	0.7317	8.1255	31.4398	78.4423	0.0384	0.8072	0.1261	0.0763
GS	0.9312	0.9247	5.1424	19.9216	49.7045	0.0191	0.9282	0.0064	0.0659
FIHS	0.9276	0.9213	5.0814	19.9604	49.8012	0.0151	0.9281	0.0072	0.0652
AIHS	0.9526	0.9462	4.3591	16.8416	42.0197	0.0109	0.9380	0.0063	0.0560
AIHS-WLS	0.9551	0.9515	4.2357	16.3586	40.8148	**0.0102**	0.9539	0.0115	0.0350
Proposed	**0.9574**	**0.9557**	**4.1228**	**16.1962**	**40.4096**	0.0236	**0.9691**	0.0134	**0.0178**

degree. The result of PCA are reddish. This is because PCA lost a lot of information. SVT and GS methods do not make full use of spatial information from the PAN image; their pansharpening results are not clear enough. The proposed method fully considers the balance between spectral information and spatial information, resulting in a pansharpening result with rich spatial details and well-preserved spectral information. The objective evaluation for this experiment is shown in Table 4. As is shown in this table, the proposed method obtains the best performance in seven evaluation metrics, which are CC, UIQI, ERGAS, RASE, RMSE, QNR, and D_s. The subjective visual effects and objective evaluation indicators demonstrate the effectiveness of the proposed method.

5 | CONCLUSION

In this paper, a multispectral remote-sensing image pansharpening method has been proposed. The proposed method utilizes GF to eliminate the influence of LFC to reduce spectral distortion. Then, the AIHS method is used to generate the initial detail map. Moreover, GF is utilized to extract spectral information and merge it into the detail map. To match the difference of different channels in MS image, the spectral information-enhanced detail map is further refined according to the adaptive coefficients. By experiments, we illustrate that the proposed method can efficiently enhance the spectral information and balance the trade-off between spectral information and spatial information. Besides, the MATLAB implementation of the proposed method will be released if this paper is accepted.

ACKNOWLEDGMENTS

The research in our paper is sponsored by National Natural Science Foundation of China (No. 61701327, No. 61711540303, No. 61473198) and Science Foundation of Sichuan Science and Technology Department (No. 2018GZ0178).

ORCID

Qilei Li https://orcid.org/0000-0002-9675-9016
Xiaomin Yang https://orcid.org/0000-0002-1094-3841
Wei Wu https://orcid.org/0000-0001-5769-9340
Gwanggil Jeon https://orcid.org/0000-0002-0651-4278

REFERENCES

1. Gebru T, Krause J, Wang Y, et al. Using deep learning and Google street view to estimate the demographic makeup of neighborhoods across the United States. *Proc Natl Acad Sci USA*. 2017;114(50):13108-13113.
2. Wu W, Anisetti M, Abdellah C, Jeon G. Image enlargement using multiple sensors. *J Sens*. 2016;2016.
3. Meng X, Shen H, Li H, Zhang L, Fu R. Review of the pansharpening methods for remote sensing images based on the idea of meta-analysis: practical discussion and challenges. *Inf Fusion*. 2019;46:102-113.
4. Simone G, Farina A, Morabito FC, Serpico SB, Bruzzone L. Image fusion techniques for remote sensing applications. *Inf Fusion*. 2002;3(1):3-15.
5. Thomas C, Ranchin T, Wald L, Chanussot J. Synthesis of multispectral images to high spatial resolution: a critical review of fusion methods based on remote sensing physics. *IEEE Trans Geosci Remote Sens*. 2008;46(5):1301-1312.
6. Mallat SG. A theory for multiresolution signal decomposition: the wavelet representation. *IEEE Trans Pattern Anal Mach Intell*. 1989;11(7):674-693.
7. Yang Y, Wan W, Huang S, Lin P, Que Y. A novel pan-sharpening framework based on matting model and multiscale transform. *Remote Sens*. 2017;9(4):391.
8. Nason GP, Silverman BW. The stationary wavelet transform and some statistical applications. In: *Wavelets and Statistics*. New York, NY: Springer-Verlag New York; 1995;281-299.
9. Shensa MJ. The discrete wavelet transform: wedding the a trous and Mallat algorithms. *IEEE Trans Signal Process*. 1992;40(10):2464-2482.
10. Zheng S, Shi W-Z, Liu J, Tian J. Remote sensing image fusion using multiscale mapped LS-SVM. *IEEE Trans Geosci Remote Sens*. 2008;46(5):1313-1322.
11. Burt PJ, Adelson EH. The Laplacian pyramid as a compact image code. In: *Readings in Computer Vision: Issues, Problem, Principles, and Paradigms*. Amsterdam, The Netherlands: Elsevier; 1987:671-679.
12. Kaplan NH, Erer I. Bilateral filtering-based enhanced pansharpening of multispectral satellite images. *IEEE Geosci Remote Sens Lett*. 2014;11(11):1941-1945.
13. Kang X, Li S, Fang L, Benediktsson JA. Pansharpening based on intrinsic image decomposition. *Sens Imaging*. 2014;15(1):94.
14. Khan MM, Chanussot J, Condat L, Montanvert A. Indusion: fusion of multispectral and panchromatic images using the induction scaling technique. *IEEE Geosci Remote Sens Lett*. 2008;5(1):98-102.
15. Scarpa G, Vitale S, Cozzolino D. Target-adaptive CNN-based pansharpening. *IEEE Trans Geosci Remote Sens*. 2018;56(9):5443-5457.
16. Vivone G, Addesso P, Restaino R, Mura MD, Chanussot J. Pansharpening based on deconvolution for multiband filter estimation. *IEEE Trans Geosci Remote Sens*. 2018:1-14.
17. Choi J, Yu K, Kim Y. A new adaptive component-substitution-based satellite image fusion by using partial replacement. *IEEE Trans Geosci Remote Sens*. 2011;49(1):295-309.
18. Al-Wassai FA, Kalyankar NV, Al-Zuky AA. The IHS transformations based image fusion. arXiv preprint arXiv:1107.4396. 2011.
19. Kwarteng AY, Chavez PS. Extracting spectral contrast in Landsat Thematic Mapper image data using selective principal component analysis. *Photogramm Eng Remote Sens*. 1989;55(3):339-348.
20. Shah VP, Younan NH, King RL. An efficient pan-sharpening method via a combined adaptive PCA approach and contourlets. *IEEE Trans Geosci Remote Sens*. 2008;46(5):1323-1335.
21. Laben CA, Brower BV, inventors; Harris Corp, assignee. Process for enhancing the spatial resolution of multispectral imagery using pan-sharpening. US Patent 6,011,875. January 4, 2000.
22. Jian L, Yang X, Wu W, Ahmad A, Sangaiah AK, Jeon G. Pansharpening using a guided image filter based on dual-scale detail extraction. *J Ambient Intell Humaniz Comput*. 2018:1-15.

23. Tu T-M, Huang PS, Hung C-L, Chang C-P. A fast intensity-hue-saturation fusion technique with spectral adjustment for IKONOS imagery. *IEEE Geosci Remote Sens Lett*. 2004;1(4):309-312.
24. Rahmani S, Strait M, Merkurjev D, Moeller M, Wittman T. An adaptive IHS pan-sharpening method. *IEEE Geosci Remote Sens Lett*. 2010;7(4):746-750.
25. Song Y, Wu W, Liu Z, Yang X, Liu K, Lu W. An adaptive pansharpening method by using weighted least squares filter. *IEEE Geosci Remote Sens Lett*. 2016;13(1):18-22.
26. Jian L, Yang X, Zhou Z, Zhou K, Liu K. Multi-scale image fusion through rolling guidance filter. *Futur Gener Comput Syst*. 2018;83:310-325
27. Chen Y, Zhang G. A pan-sharpening method based on evolutionary optimization and IHS transformation. *Math Probl Eng*. 2017;2017.
28. He K, Sun J, Tang X. Guided image filtering. In: *Computer Vision - ECCV 2010: 11th European Conference on Computer Vision, Heraklion, Crete, Greece, September 5-11, 2010, Proceedings, Part I conference on computer vision*. Berlin, Germany: Springer-Verlag Berlin Heidelberg; 2010;1-14.
29. Nejati M, Samavi S, Shirani S. Multi-focus image fusion using dictionary-based sparse representation. *Inf Fusion*. 2015;25:72-84.
30. Wald L, Ranchin T, Mangolini M. Fusion of satellite images of different spatial resolutions: assessing the quality of resulting images. *Photogramm Eng Remote Sens*. 1997;63(6):691-699.
31. Alparone L, Wald L, Chanussot J, Thomas C, Gamba P, Bruce LM. Comparison of pansharpening algorithms: outcome of the 2006 GRS-S data-fusion contest. *IEEE Trans Geosci Remote Sens*. 2007;45(10):3012-3021.
32. Wang Z, Bovik AC. A universal image quality index. *IEEE Signal Process Lett*. 2002;9(3):81-84.
33. Wald L. Quality of high resolution synthesised images: is there a simple criterion? Paper presented at: The Third Conference ''Fusion of Earth Data: Merging Point Measurements, Raster Maps and Remotely Sensed Images'' (SEE/URISCA); 2000; Sophia Antipolis, France.
34. Choi M. A new intensity-hue-saturation fusion approach to image fusion with a tradeoff parameter. *IEEE Trans Geosci Remote Sens*. 2006;44(6):1672-1682.
35. Chang C-I. Spectral information divergence for hyperspectral image analysis. In: Proceedings of the IEEE 1999 International Geoscience and Remote Sensing Symposium, Vol. 1 (IGARSS); 1999; Hamburg, Germany.
36. Alparone L, Aiazzi B, Baronti S, Garzelli A, Nencini F, Selva M. Multispectral and panchromatic data fusion assessment without reference. *Photogramm Eng Remote Sens*. 2008;74(2):193-200.

How to cite this article: Li Q, Yang X, Wu W, Liu K, Jeon G. Pansharpening multispectral remote-sensing images with guided filter for monitoring impact of human behavior on environment. *Concurrency Computat Pract Exper*. 2021;33:e5074. https://doi.org/10.1002/cpe.5074